5 (2025) 100048

Contents lists available at ScienceDirect

Materials Chemistry and Physics: Sustainability and Energy

journal homepage: www.sciencedirect.com/journal/materials-chemistry-and-physics-sustainability-and-energy

Synergistic antibacterial activity of green-synthesized Ag-Fe-Zn trimetallic nanocomposites using Tinospora cordifolia leaf extract

Greeshma Sunkari [a], Saroj Vijaylakshmi [a,g], ML Sowjanya [a,d,e], Vasamsetti Sai Madhuri [b], Naveen Kumar Madipoju [a], Naveen Kumar Dabbeta [a], Prince Kumar [c], Pranay Bhasker Kalakonda [h], Likhith Chandan Kalakonda [a,f], Vijay Morampudi [b], Suryanarayana Jammalamadaka [c], Parvathalu Kalakonda [a,*]

[a] Department of Physics, Smart Nanomaterial Research Laboratory (SNRL), Government City PG College (A), Osmania University, Hyderabad, TG, 500002, India
[b] Department of Biochemistry, University of Hyderabad, Hyderabad, TG, 500046, India
[c] Department of Physics, Indian Institute of Technology, Hyderabad, TG, 502284, India
[d] Department of Physics, National Institute of Technology, Warangal, TG, 506004, India
[e] St.Joseph's Degree and PG College, Hyderabad, TG, 500001, India
[f] FIITJEE World School, Dilsukhnagar, Hyderabad, TG, 500036, India
[g] Department of Physics, Dayananada Sagar University, Bangalore, KA, 560078, India
[h] Department of Materials Science and Engineering, North Carolina State University, Raleigh, NC, 27695, USA

A R T I C L E I N F O

Keywords:
Trimetallic nanoparticles
Biosynthesis
Antipathogenic
EPEC
Magnetic properties

A B S T R A C T

Silver-iron-zinc trimetallic nanocomposites (Ag-Fe-Zn TMNCs) were synthesized via a one-step, eco-friendly process utilizing Tinospora cordifolia (TC) leaf green extract as a versatile multifunctional agent. Silver nitrate, iron oxide (III), and zinc nitrate served as precursor materials for the trimetallic nanocomposite formation. Comprehensive characterization was performed using XRD, UV–Vis, FTIR, FE-SEM, EDS, VSM, and Zetasizer. FTIR spectra confirmed the presence of bio-functional groups from the TC extract on the surface of the metal nanocomposites (MNPs), while SEM and XRD analyses confirmed the topology and multi-phase crystalline structure of the TMNCs, dominated by a cubic spinel $ZnFe_2O_4$ phase. Zetasizer results indicated enhanced colloidal stability for the TMNCs and VSM measurements demonstated magnetic behaviour. The antimicrobial activity of the synthesized TMNCs was evaluated against Escherichia coli (EPEC) and probiotic Lactobacillus (Lb) through growth and viability assays, using Gentamicin as a reference standard antibiotic. The Ag-based bimetallic nanoparticles (BMNPs) and Ag-Fe-Zn TMNCs exhibited superior antibacterial activity compared to their monometallic counterparts, with 1:1:1 Ag-Fe-Zn TMNCs showing the strongest inhibition, likely due to enhanced synergistic interactions at the bacterial membrane interface. Notably, AgNPs, Ag-Zn BMNPs, Ag-Fe BMNPs, and Ag-Fe-Zn TMNCs demonstrated significant inhibitory effects against pathogenic EPEC and probiotic Lb, whereas FeNPs and Zn-Fe BMNPs selectively inhibited EPEC without affecting probiotic Lb. The Ag-Fe BMNPs and Ag-Fe-Zn TMNCs exhibit magnetic properties, suggesting potential for future exploration in targeted therapeutic applications in addition to their robust antibacterial activity. These findings highlight the potential of green-synthesized Ag-Fe-Zn TMNCs as potent, multifunctional agents for biomedical and antibacterial industrial applications.

1. Introduction

The rapidly evolving field of bio-nanotechnology bridges diverse disciplines across basic sciences and engineering, with metal nanoparticles exhibiting unique properties that enable a variety of biomedical and pharmaceutical industrial applications, including potential solution for targeted drug delivery using external magnetic fields for antibacterial therapies [1–3]. Metal nanoparticles synthesized through a variety of techniques demonstrate remarkable versatility, finding applications in pharmaceutical formulations, targeted delivery

* Corresponding author.
E-mail addresses: parvathalu.k@gmail.com, parvathalu@wpi.edu (P. Kalakonda).

https://doi.org/10.1016/j.macse.2025.100048
Received 12 July 2025; Received in revised form 13 October 2025; Accepted 14 October 2025
Available online 14 October 2025

systems for anticancer and antimicrobial agents, as well as in energy storage, agriculture, sensing technologies, and advanced materials for smart electronics [4–7]. Due to the health concerns linked to traditional antibiotics and the growing problem of antimicrobial resistance, there is a pressing demand to develop novel antimicrobial agents. Special attention is being given to alternatives produced through an eco-friendly synthesis methods, as these may offer effective ways to treat infections and address global health challenges [8–10]. To address the growing demand for safer antimicrobial strategies and reduce global health risks, green-synthesized mono metal nanoparticles (MMNPs), bimetallic nanoparticles (BMNPs) [11–13], and trimetallic nanoparticles (TMNCs) have emerged as highly promising alternatives to conventional antibiotics for targeted antibacterial applications [14–18].

The strategic selection of constituent metals is critical to designing TMNCs with enhanced functionality. In this study, silver (Ag), iron (Fe), and zinc (Zn) were chosen leverage their unique and synergistic attributes. AgNPs are renowned for their potent antibacterial action, primarily mediated through the disruption of microbial cell membranes and the induction of oxidative stress [19]. FeNPs contribute essential ferrimagnetic behavior, which is fundamental for applications in magnetically guided targeting and drug delivery [20,21]. ZnNPs not only exhibit inherent antimicrobial properties but also enhance the stability of the nanocomposite [16,22,23]; significantly, formulations containing ZnNPs have demonstrated the efficacy to selectively inhibit pathogenic bacteria while exhibiting minimal effects on beneficial probiotic strains [24]. The confluence of these three metals is designed to produce a synergistic enhancement, yielding a multifunctional agent with superior antibacterial potency, selective action, and capabilities for targeted therapy. Recent research and technology have focused on developing environmentally benign and cost-effective methods for synthesizing metal nanoparticles (MNPs) [25–27]. A variety of synthesis techniques are currently employed for the fabrication of metal nanoparticles [28], including chemical reduction, microwave-assisted processes, and biosynthetic techniques utilizing plant materials such as leaves, fruits, and peels [29–31]. Chemical synthesis methods for metal nanoparticles often involve complex procedures and significant financial investment, which can result in toxic byproducts, environmental hazards, and potential health risks, including compromised immune function in humans [32–37].

Metal nanoparticles are widely utilized in bio-nanotechnology owing to their diverse multifunctional properties [38]. The integration of magnetic nanoparticles with those exhibiting strong optical, catalytic, and thermoelectric characteristics enhances targeted drug delivery, sensing, and antimicrobial applications, primarily due to their high surface-to-volume ratio and the synergistic interactions among different nanoparticles [39–44]. Previously, mono and bimetallic nanoparticles (BMNPs) have been studied as potential antibacterial agents due to their core shell structures and synergistic effect between the constituent ions [21,45–47]. Recently, various bimetallic combinations have been used to study potential antibacterial activity and sustainable water purification process as a part recycling of used water [48–51]. BMNPs showed greater potential antibacterial activity compared to monometallic nanoparticles owing to the enhanced energy afforded by the presence of two metal ions [19,52–56].

In this study, we report for the first time, the synthesis of Ag-Fe-Zn TMNCs using a green extract from medicinal TC leaves and evaluated their antibacterial properties against both EPEC pathogen and Lb probiotic. While previous research has explored the synthesis and antimicrobial properties of mono- and bimetallic nanoparticles, the eco-friendly fabrication of TMNCs employing TC plant leaf extract remains unexplored. The TC plant is particularly notable for its medicinal value and its effectiveness as a capping and stabilizing agent during the nanoparticle synthesis process. Herein, Ag-Fe-Zn TMNCs were synthesized via a green route, and their antibacterial efficacy was systematically assessed through disc diffusion and growth viability assays. Additionally, the magnetic properties of both BMNPs and TMNCs were investigated to demonstrate their potential utility in targeted drug delivery applications under an external magnetic field. Our findings highlight the promise of synthesized Ag-Fe-Zn TMNCs as potent antibacterial agents and underscore the advantages of this green, energy-efficient, and cost-effective approach for scalable production, with broad implications for commercial biomedical and industrial applications.

2. Methods and characterizations

2.1. Materials

Iron(III) oxide (Fe_2O_3), silver nitrate ($AgNO_3$), Zinc nitrate ($Zn(NO_3)_2$) and all other basic solvents were procured from Sigma-Aldrich Pvt.Ltd, Hyderabad, India. The TC fresh leaves were collected from the medicinal garden, Hyderabad, TG, India.

2.2. Synthesis of nanoparticles

The biosynthesis method used in this study is based on our earlier research [37]. For the preparation of TMNPs, 100 mL of green extract from TC leaves was gradually introduced into a 1:1:1 mixture of $AgNO_3$, $Zn(NO_3)_2$, and Fe_2O_3 salts in a 300 mL beaker using a standard burette. The 1:1:1 metal salt ratio was selected based on the molarity of the metal ion precursors. The synthesis was conducted under controlled conditions: a temperature of 90 °C, stirring at 800 rpm, and a reaction time of 1 h. After synthesis, the filtered or washed nanoparticles were dried in an oven to obtain a fine powder. Fig. 1 illustrates the overall biosynthesis process, and each experiment was performed in triplicate to ensure reproducibility.

2.3. Characterization of synthesized nanoparticles

The formation of TMNCs was confirmed using UV–visible spectroscopy. FTIR was employed to identify the surface bio-functional groups that are responsible for the nucleation & growth of NPs. SEM and EDS were utilized to characterize surface topology and the elemental composition of the sample. The phase and crystallite size of the NPs were estimated using XRD analysis. The magnetic properties of the nanocomposites were assessed with a vibrating sample magnetometer (VSM), while the colloidal stability was evaluated based on zeta potential measurements. These characterizations encompassed the NPs their optical properties, magnetic properties, chemical composition, morphology, and crystal phase details.

2.4. Antibacterial activity

The antimicrobial activity of the NPs, including mono/BMNPs/Ag-Fe-Zn TMNCs was processed within a clean sterile laboratory, using a biosafety cabinet and the procedure is mentioned in our previous research work [47]. To ensure reliability, the antibacterial activity assays against both EPEC and probiotic Lactobacillus (Lb) were performed in triplicate.

2.4.1. Bacterial culture

The pathogenic organism used was EPEC, and the probiotic organism was Lb. EPEC was grown in LB (Luria Bertani) broth, while Lb was cultivated in De Man-Rogosa-Sharpe (MRS) broth. Both cultures were incubated overnight at 37 °C in an incubator shaker. Overnight cultures were adjusted to an optical at OD1 at 600 nm for use in assays.

2.4.2. Evaluating antibacterial activity of NPs using disc diffusion, bacterial growth and viability assays

The antibacterial activity of the NPs, including mono, BMNPs and TMNCs, was estimated against EPEC and gram-positive probiotic Lb using disc diffusion, and bacterial viability assays. A 30 μg concentration

Fig. 1. Biosynthesis process of TC leaf extracts mediated mono/bi/TMNCs.

of monometallic nanoparticles (AgNPs, ZnNPs, FeNPs), bimetallic nanoparticles (Ag-Zn, Ag-Fe, Zn-Fe BMNPs) and trimetallic nanoparticles (Ag-Zn-Fe TMNCs) were incubated with 10^7 CFU of EPEC and Lb in 100 μl of respective media Luria Bertani (Lb) for EPEC and De Man-Rogosa-Sharpe (MRS) for Probiotic (Lb) bacterial strains for 6 h at 37 °C. untreated EPEC and untreated Lb were used as the negative controls and Gentamicin was used as the positive control to test the antimicrobial effect. The growth kinetics of both the EPEC and Lb strains were determined before and after incubation with nanoparticles by measuring their optical density values at a wavelength of 600 nm. Following the disc diffusion assay, where 30 μg of the NPs were dried on the disc and placed on the Petri plates overlaid with EPEC pathogen and the diameter of the clear zone of inhibition around each disc was measured to quantify the inhibitory effect of the nanoparticles.

To investigate the bacterial growth and viability in the presence of nanoparticles, cultures of EPEC and Lb were adjusted to an inoculum of 10^7 CFU in 100 μl of their respective media and incubated with mono, BMNPs and TMNCs at a concentration of 30 μg/ml for 6 h at 37 °C. Untreated EPEC and Lb were kept as negative controls and Gentamicin (30 μg) was used as a reference positive control, while sterile LB broth served as the blank control. All samples were diluted serially up to 10, 100, 1000, 10,000, and 1,00,000-fold dilutions; then 10 μl of each was plated on respective agar plates and incubated at specified conditions. The bacterial growth and viability of NPs bacterial activity were quantified by the colony number per dilution and compared to untreated EPEC and Lb controls. After the incubation period, colonies were counted and growth of EPEC and Lb was determined by colony forming unit (CFU) counts. The efficacy and safety profile of the TMNCs should be further explored through cytotoxicity assays and in vivo studies to better understand their anti-pathogenic activity.

3. Results

3.1. UV–VIS spectroscopy

The UV–Vis absorption spectrum of the Ag-Fe-Zn TMNCs synthesized using TC leaf extract is presented in Fig. 2. The spectra were collected in the wavelength range of 250–700 nm. The TMNCs spectrum exhibits a broad absorption band centered around 330–530 nm, with a shoulder peak absorption on the lower wavelength side (~280–380 nm for FeNPs). The highest absorbance value is observed at the short-wavelength end (270–320 nm), followed by a decrease and stabilization between 330 and 530 nm. The broad nature of the absorption band suggests the successful formation of TMNCs, with possible overlapping surface plasmon resonance (SPR) peaks corresponding to AgNPs, FeNPs, and ZnNPs. Typically, AgNPs exhibit SPR peaks around 400–530 nm, while FeNPs (280 nm) and ZnNPs (350 nm) contribute to absorption in the UV region. The observed absorption features suggest the formation of Ag-Fe-Zn TMNCs. The broadening and slight shift of the SPR band compared to monometallic nanoparticles indicate possible synergistic interactions and complexation process among the three metals, influenced by the capping effect of phytochemicals from the TC extract.

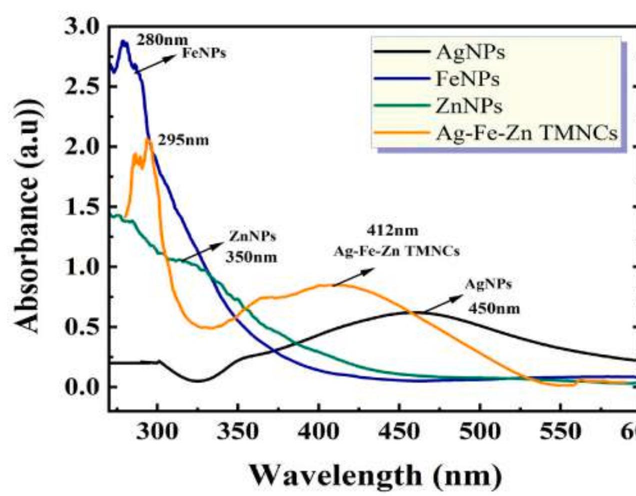

Fig. 2. UV–Vis absorption spectrum of AgNPs, FeNPs, ZnNPs and Ag-Fe-Zn trimetallic nanocomposites (TMNC) synthesized with TC leaf extract.

3.2. Fourier transform infrared spectroscopy (FTIR)

The FTIR spectra of AgNPs, FeNPs, ZnNPs, and Ag-Fe-Zn TMNCs synthesized using TC leaf extract reveals distinct functional groups and metal-oxygen bonds, confirming successful nanoparticle formation and stabilization. The IR spectra, as shown in Fig. 3, shows that all samples exhibit a broad O-H stretching band at approximately 3400 cm^{-1}, indicating the presence of O-H groups from plant phytochemicals [57]. This band is characteristic of phenolic compounds and polysaccharides, which are abundant in TC extract [58] and these compounds are well-known for their role in the reduction & stabilization of metal ions of NPs through hydrogen bonding. A strong C=O stretching near 1630 cm^{-1} is observed in all spectra [58], suggesting the involvement of carbonyl-containing compounds in nanoparticle capping and stabilization. For the monometallic nanoparticles, characteristic Zn-O and Fe-O stretching vibrations appear below 600 cm^{-1} in ZnNPs and FeNPs, respectively, while AgNPs show prominent O-H and C=O stretches [19]. Notably, the Ag-Fe-Zn TMNCs spectrum exhibits both Zn-O and Fe-O stretching bands below 600 cm^{-1}, along with a distinct C-N stretching band around 1380 cm^{-1}, indicating the synergistic integration of all three metals and the enhanced interaction with plant-derived amine groups. These results collectively confirm the successful green synthesis and stabilization of monometallic (MNPs) and trimetallic nanoparticle composites (TMNCs) by TC extract.

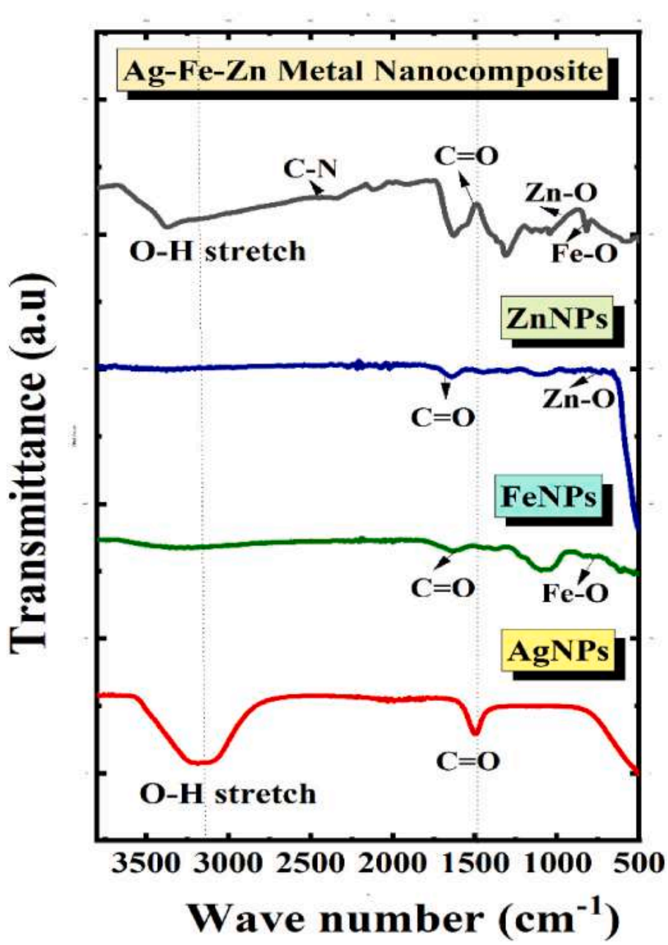

Fig. 3. FTIR spectra of TC leaf extract mediated AgNPs, FeNPs, ZnNPs and Ag-Fe-Zn TMNCs.

3.3. Scanning electron microscopy (SEM) and energy dispersive spectroscopy (EDS)

The morphology and size of the Ag-Fe-Zn TMNCs were examined using FE-SEM, which revealed densely aggregated structures with primary clusters measuring approximately **120 nm** (Fig. 4 A and B). For comparison, the average hydrodynamic diameter of the particles in suspension was determined to be **181.8** $\pm$ **16.6** nm via Zetasizer analysis. This larger hydrodynamic size is typical for nanoparticles stabilized by a **biological capping agent**, as the measurement includes the layer of phytochemicals from **the extract surrounding the metal core**. The significant difference between the dry-state cluster size (SEM) and the hydrated dynamic diameter (Zetasizer) is well-established and accounts for the solvation layer and the inherent principles of each technique. The formation of these aggregated sheet structures and clusters may be attributed to different crystal growth kinetics and complexation of the three metal nano particles Ag, Fe, Zn. The EDS spectrum (Fig. 4C) confirms the presence of silver, iron, and zinc as the main elements. The quantitative analysis (Fig. 4 D) reveals iron as the predominant component (52.91 wt%), followed by silver (32.47 wt%) and zinc (14.62 wt%). The observed elemental composition deviates from the initial stoichiometry primarily due to the distinct reduction potential of the metal ions. Silver ions (Ag^{+}), possessing a higher reduction potential, are preferentially reduced and incorporated over iron (Fe^{3+}) and zinc (Zn^{2+}) ions, leading to an enriched silver content in the final nanocomposite. This combination of morphological diversity and well-defined elemental composition demonstrates the successful and uniform integration of all three metals in the nanocomposite material (TMNCs). Uniquely, the biosynthesis process yielded a trimetallic system with a notably high iron content, distinguishing these nanocomposites from previously reported plant-mediated systems.

3.4. X-RAY diffraction (XRD)

The XRD profile of the NPs confirms the crystalline nature and phase composition of AgNPs, FeNPs, ZnNPs, and the Ag-Fe-Zn trimetallic nanocomposite (TMNCs) (Fig. 5). For AgNPs, distinct peaks at 2θ values of approximately 38.1°, 44.3°, and 64.5° correspond to the (111), (200), and (220) planes of an FCC structure (PDF: 01-090-7293) [59], while FeNPs display broad reflections at 35.6°, 43.2°, 57.1°, and 62.7°, indexed to the (311), (400), (511), and (422) planes (PDF: 04-006-9059), which are characteristic of the spinel phase of iron oxide. ZnNPs show sharp peaks at 31.7°, 34.4°, 36.2°, 47.5°, and 56.6°, attributable to the (100), (002), (101), (102), and (110) (PDF: 04-004-4120) planes of hexagonal wurtzite zinc oxide [60,61].

X-ray diffraction analysis of the Ag-Fe-Zn trimetallic nanocomposite shows that $ZnFe_2O_4$ (JCPDS: 00-022-1012) [62,63] is the dominant crystalline phase, as indicated by strong reflections from the (220), (311), (222), (400), (422), (511), and (440) planes (Fig. S1), characteristic of the cubic spinel structure with Zn^{2+} ions primarily occupying tetrahedral sites and Fe^{3+} ions in octahedral sites, forming a normal spinel arrangement [64]. The intensity of these 7 peaks confirms high crystallinity and phase purity of $ZnFe_2O_4$ (87.7 % from PA Nalytical X'Pert high score software), while the broadening of peaks in the composite indicates nanoscale crystallite size. This size was estimated using the Scherrer equation to be in the nanometer range typically 10–25 nm [28]. Uniquely, the TMNCs pattern displays additional peak overlap and intensity modulation, reflecting synergistic interactions among the three metal components and the formation of a well-integrated, multi-phase nanocomposite (Zinc oxide (ZnO, 4.4 %, Metallic silver (Ag, 1.1 %, $Fe_{\sim 2.67 \sim}O_4$, 1.4 %) that is distinct from the individual monometallic nanoparticles (Fig. S2). This structural integration is expected to impart enhanced physicochemical and antibacterial properties to the TMNCs, setting them apart from their monometallic analogs. The crystalline size details of the Ag-Fe-Zn TMNCs are shown in Table .1.

The crystallite size (D) was calculated using the Debye Sherrer

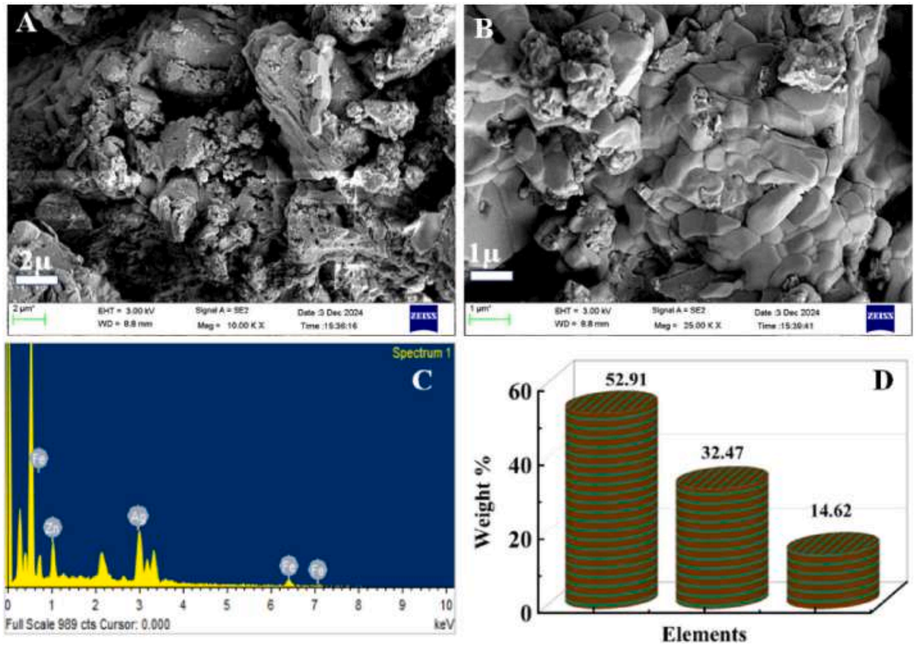

Fig. 4. (A, B) FE-SEM images of Ag-Fe-Zn trimetallic nanocomposites (TMNCs) showing aggregated and irregular morphology; (C) EDS spectrum confirming the presence of Ag, Fe, and Zn elements in the TMNCs; (D) Quantitative elemental composition of the composite sample.

equation: $D = K\lambda/(\beta\ \cos\theta)$. This analysis confirms that the nanocomposite is nanocrystalline, with an average crystallite size of approximately **13.2** nm, which is consistent with the broadened peaks observed in the XRD pattern. The variation in size between different phases and planes is expected due to differences in crystal growth kinetics and the complex multiphase nature of the composite.

3.5. Zeta potential

The Fig. 6 illustrates the zeta potential values for different nanomaterials, showing that all samples possess negative surface charges, which is indicative of electrostatic stability in colloidal suspensions [65,66]. Among the materials, monometal nanoparticles (AgNPs, FeNPs, ZnNPs) exhibit moderately negative zeta potentials, with FeNPs having the least negative value. In contrast bimetallic nanoparticles (Ag-Zn BMNPs, Ag-Fe BMNPs, Zn-Fe BMNPs) display increasingly negative values (−20 to −30mV), suggesting that these composites have good colloidal stability. The trimetallic nanocomposite (Ag-Fe-Zn TMNCs) demonstrates the most negative zeta potential, approaching −30 mV, which implies good colloidal stability among the tested materials. This superior stability is attributed to stronger electrostatic repulsive forces associated with higher absolute zeta potential values, which effectively reduce the risk of aggregation in suspension.

3.6. Vibrating sample magnetometry (VSM)

Magnetic behavior of all the TC leaf extract mediated Ag-Zn BMNPs, Ag-Fe BMNPs and Ag -Fe-Zn TMNCs were characterized using a vibrating sample magnetometer (VSM) (Make Lakeshore 8404) [67]. It is evident from Fig. 7 that magnetization measurements were performed in the magnetic field range of −2 T to +2 T (a 10 mg sample was used for measurements). The magnetization of Ag-Fe BMNPs and Ag-Fe-Zn TMNCs did not saturate at the maximum magnetic field. Nevertheless, the presence of an open hysteresis loop at the origin (inset) indicates ferrimagnetic behavior with a low coercivity of ~20 Oe for both the Ag-Fe BMNPs and Ag-Fe-Zn TMNCs. In contrast, Ag-Zn BMNPs composite exhibits diamagnetic behavior. It is also clear from Fig. 7 that the magnetization value of Ag-Fe BMNPs is marginally higher than that of Ag-Fe-Zn TMNCs, which may be due to the presence of Zn in the latter composite. As they exhibit reasonably good magnetic characteristics, these composites may be useful for the targeted drug delivery applications in addition to antibacterial applications. The magnetic behavior of these composites, combined with their antibacterial efficacy, positions them as promising candidates for future research into magnetically guided therapies.

3.7. Antibacterial activity of nanoparticles

3.7.1. Disc diffusion assay

The disc diffusion assay results depicted in Fig. 8 and Fig. 9 demonstrate that all tested nanomaterials exhibit zones of inhibition against EPEC bacteria, indicating antibacterial activity, with the size of the clear zones varying among the samples. Notably, the Ag-Fe-Zn trimetallic nanocomposites (TMNCs) produce the largest inhibition zone, suggesting superior antibacterial efficacy compared to both single-metal nanoparticles [11,17,27,45,48,52,64,67] (AgNPs, ZnNPs, and FeNPs) and bimetallic nanoparticles (Ag-Zn BMNPs, Ag-Fe BMNPs, and Zn-Fe BMNPs) [68–71]. In contrast, the control discs with PBS and untreated EPEC show no inhibition, confirming the specificity of the nanomaterials' antibacterial action. These results highlight the enhanced antibacterial potential achieved through the combination of multiple metals, particularly in the trimetallic formulation.

3.7.2. ANTT-BACTERIAL pathogenic growth activity

Antibacterial screening demonstrated that silver-based nanoparticles and their combinations (AgNPs, Ag-Zn BMNPs, Ag-Fe BMNPs, and Ag-Fe-Zn TMNCs) exerted strong inhibitory effects on the growth of the pathogenic EPEC strain, achieving reductions in bacterial density comparable to Gentamicin (Fig. 10). FeNPs and the Zn-Fe BMNPs also suppressed EPEC growth, though their effects were somewhat less pronounced, while ZnNPs alone did not significantly impact EPEC under the tested conditions. In contrast, the beneficial Lactobacillus (Lb) strain was highly sensitive to AgNPs, Ag-Fe BMNPs, and Ag-Fe-Zn TMNCs, but remained unaffected by FeNPs and Zn-Fe BMNPs. These results highlight that while Ag-containing nanoparticles provide broad-spectrum antibacterial activity against both harmful and beneficial bacteria, FeNPs and Zn-Fe BMNPs offer a more selective approach, effectively targeting EPEC while sparing probiotic Lactobacillus. This selective inhibition

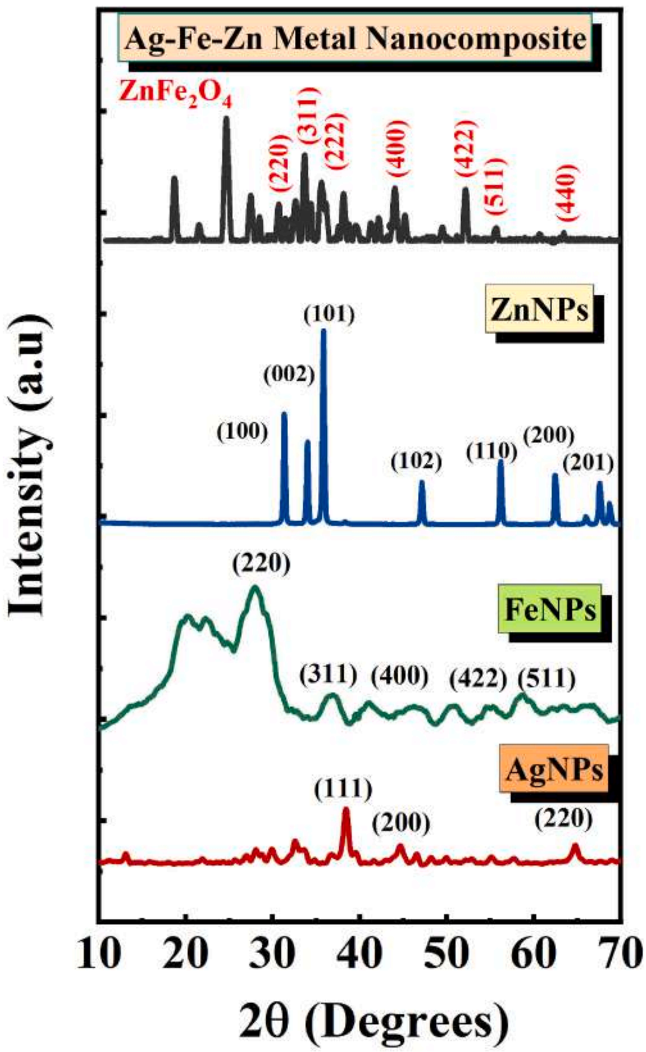

Fig. 5. XRD spectra of TC leaf extract mediated AgNPs, FeNPs, ZnNPs and Ag-Fe-Zn TMNCs.

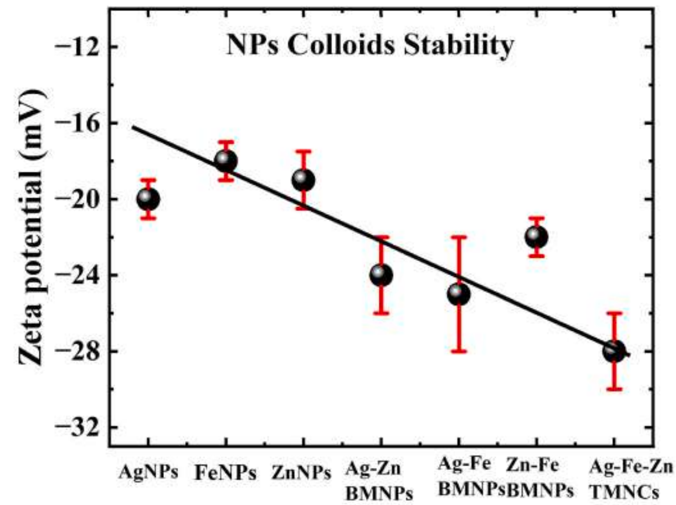

Fig. 6. Zeta potential of TC leaf extract mediated AgNPs, FeNPs, ZnNPs and Ag-Fe-Zn TMNCs.

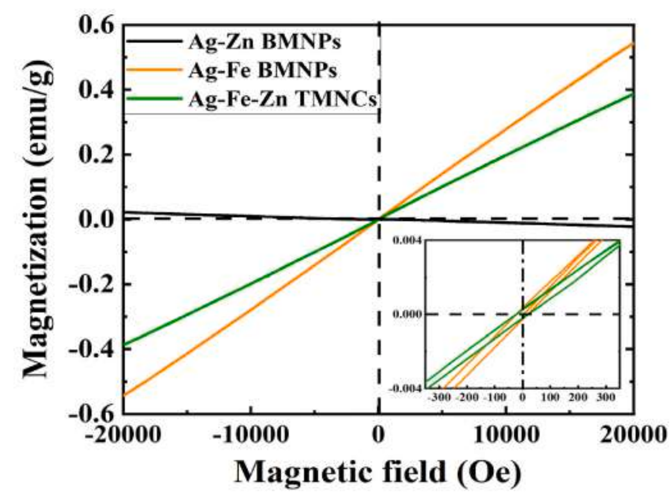

Fig. 7. VSM spectra of TC leaf extract mediated Ag-Zn BMNPs, Ag-Fe BMNPs and Ag-Fe-Zn TMNCs.

Table-1
Crystallite size calculation for Ag-Fe-Zn TMNCs using the Debye-Scherrer equation.

Phase	hkl Plane	2θ (deg)	FWHM (β) (deg)	FWHM (β) (rad)	Crystallite Size, D (nm)
$ZnFe_2O_4$	(311)	35.58	0.689	0.0120	12.8
$ZnFe_2O_4$	(400)	43.22	0.612	0.0107	14.9
$ZnFe_2O_4$	(511)	57.12	0.734	0.0128	12.9
$ZnFe_2O_4$	(440)	62.72	0.592	0.0103	16.6

suggests that FeNPs and Zn-Fe BMNPs may be preferable for applications where preservation of beneficial microbiota is desired alongside pathogen control. The antipathogenic activity of nanomaterials against EPEC and beneficial Lactobacillus (Lb) are shown in Table .2.

3.7.3. Bacterial growth and viability assay

Assessment of bacterial growth and viability by colony forming unit (CFU) analysis revealed distinct antimicrobial responses of EPEC and Lactobacillus (Lb) to various nanoparticles. Silver-based NPs including AgNPs, Ag-Zn BMNPs, Ag-Fe BMNPs, and Ag-Zn-Fe TMNCs produced a significant reduction in EPEC CFU counts, achieving inhibition comparable to that of Gentamicin, as shown in both the spot dilution plates (Fig. 11) and bar graphs (Fig. 12). In contrast, ZnNPs alone did not significantly affect EPEC viability, while FeNPs,Zn-Fe BMNPs selectively inhibited EPEC without affecting probiotic Lb (as directly shown in the CFU counts in Fig. 12); Ag-Fe-Zn TMNCs demonstrated a more favorable selectivity profile compared to other Ag-containing formulations. For Lb, Ag-containing NPs also resulted in a drastic decrease in CFU, indicating broad-spectrum antibacterial action, whereas FeNPs, ZnNPs, and Zn-Fe BMNPs did not compromise Lb viability, maintaining high CFU levels similar the untreated control. These results demonstrate that Ag-based NPs are effective against both pathogenic and probiotic bacteria, while FeNPs and Zn-Fe BMNPs selectively inhibit EPEC without harming beneficial Lb, supporting their potential for targeted antimicrobial strategies that preserve the probiotic population.

4. Discussion

Various combinations of MNPs have shown promise as antibacterial agents for addressing the range of persistent infections. Integrating different BMNPs/TMNCs metal ions into BMNPs & TMNCs hybrid nanocomposites has enabled researchers to explore their synergistic effects, resulting in enhanced physicochemical properties and superior antimicrobial performance. In this work, we focused on comparing the

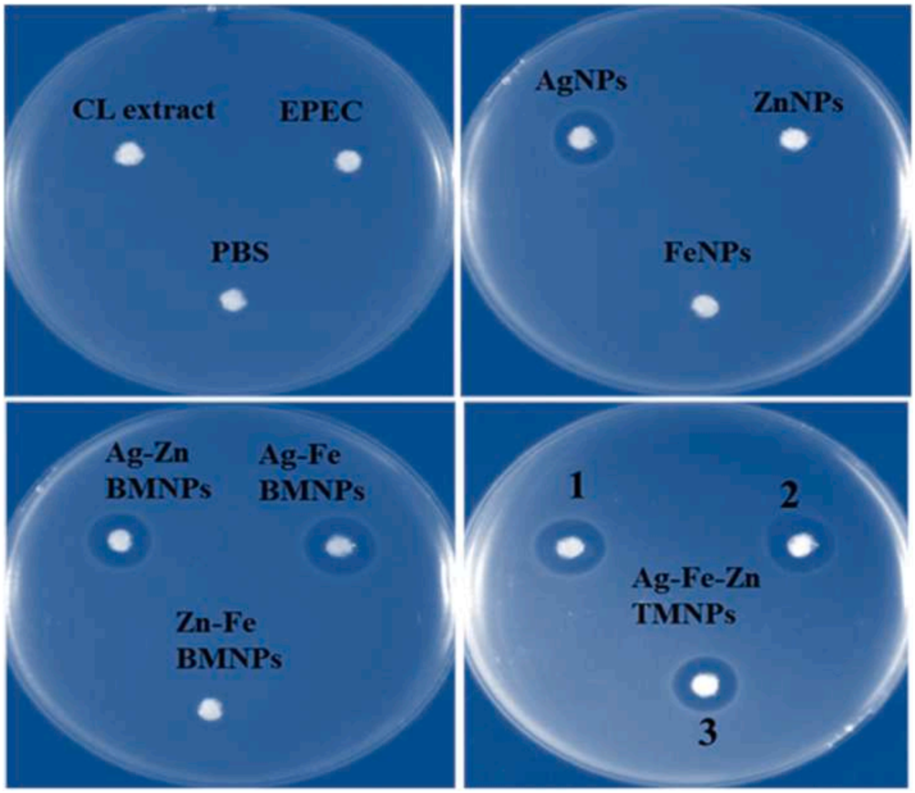

Fig. 8. Antibacterial activity of TC mediated Ag-Fe-Zn TMNCs on EPEC via disc diffusion assay.

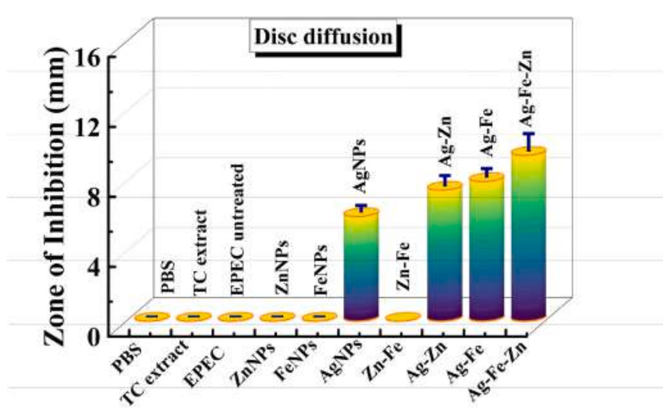

Fig. 9. Zone of inhibition of extract/untreated EPEC/mono/BMNPs/TMNCs nanomaterials via disc diffusion assay.

antibacterial activity of mono/BMNPs/TMNCs against both EPEC and probiotic Lb. The optical, magnetic and structural properties of the mono/BMNPs/TMNCs were examined thoroughly using different characterization techniques. The successful synthesis of TMNCs was verified by UV–Vis absorption spectroscopy, which revealed broad absorption spectra. Further analysis using XRD and FTIR provided evidence of their

Table 2
Antipathogenic activity of nanomaterials against EPEC and beneficial Lactobacillus (Lb).

S.No	% inhibition of EPEC	% inhibition of Lb
AgNps	44.54767726	69.75438596
ZnNPs	37.55501222	0
FeNPs	15.94132029	0
Ag- Zn Nps	60.97799511	43.68421053
Ag- Fe Nps	88.60635697	88.45614035
Zn- FeNps	45.13447433	0
Ag-Zn- Fe Nps	84.05867971	94.38596491
Gentamicin	81.27139364	29.40350877

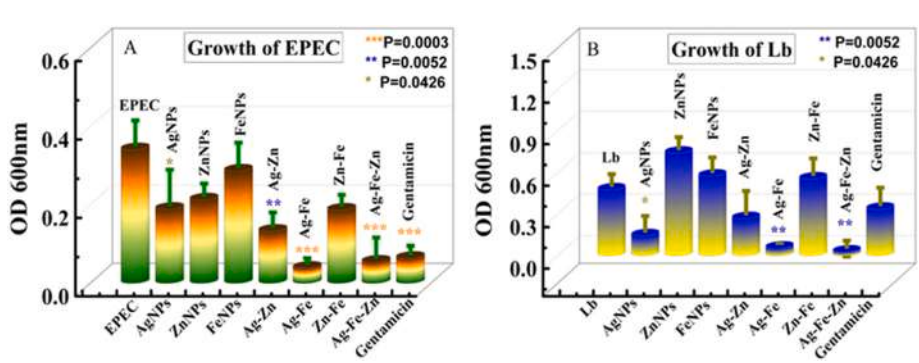

Fig. 10. Antibacterial pathogenic growth activity against EPEC and Lb probiotic as the function of mono/BMNPs and TMNCs.

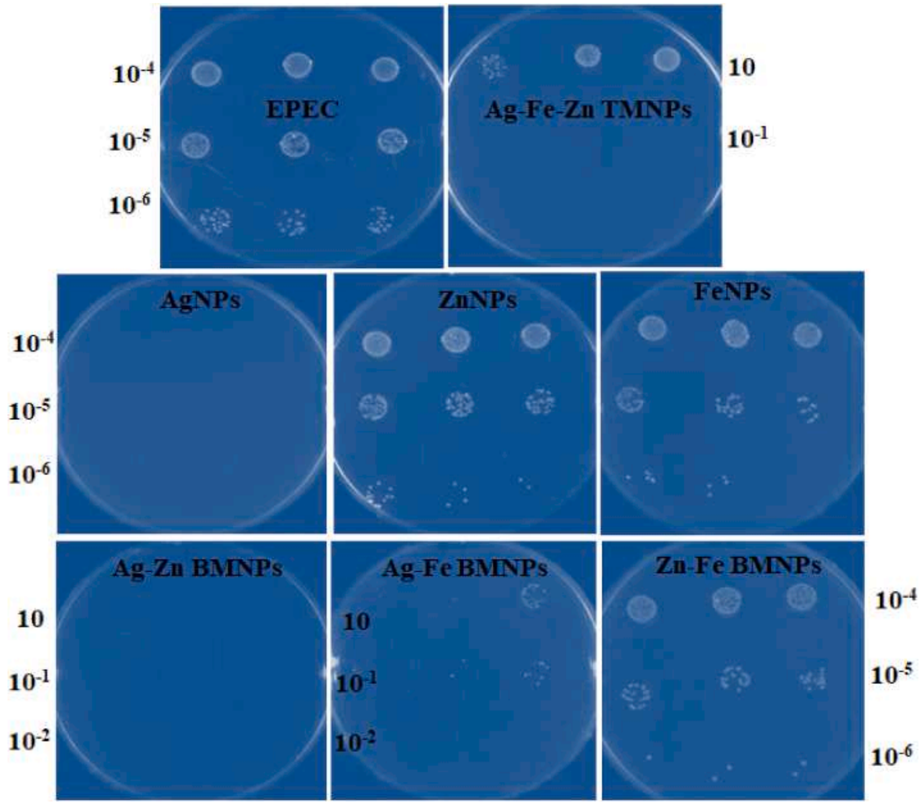

Fig. 11. Bacterial growth and viability test against EPEC as a function of mono/BMNPs and TMNCs.

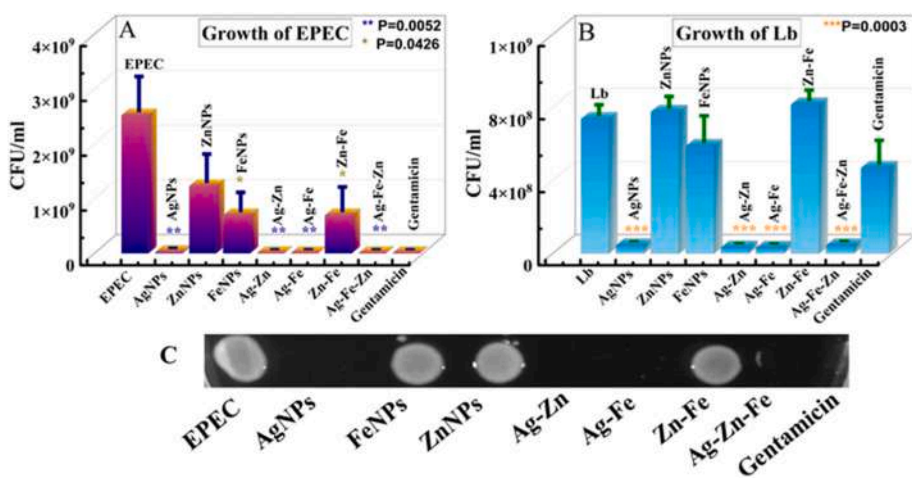

Fig. 12. Bacterial growth and viability test against EPEC and Lb as the mono/BMNPs and TMNCs.

crystalline nature and revealed the bio-functional groups on the surface the NPs. VSM analysis confirmed the ferrimagnetic behaviour of the composite, consistent with the presence of $ZnFe_2O_4$ identified as one of the ferrimagnetic phases within the material. Importantly, the use of TC leaf green extract played a crucial role in directing the assembly of complex nanostructures, while also significantly boosting the antibacterial efficacy of the resulting nanocomposite.

The antibacterial activity of mono/BMNPs/TMNCs was studied against both EPEC and Lb and the standard antibiotic Gentamicin was used as a reference. The results show that the Ag-Fe-Zn TMNCs exhibited significantly higher antimicrobial activity against both EPEC and Lb [47]. The improved antibacterial activity of Ag-Fe-Zn TMNCs can be attributed to the synergistic effects arising from the incorporation of different metal ions present in the composite. The XRD and SEM data indicate a composite structure, not a core-shell. We hypothesize that the Fe/Zn oxide matrix acts as a scaffold, preventing the aggregation of Ag NPs (as seen in Zeta potential data). This improved dispersion increases the available surface area of Ag, potentially enhancing its biological activity. To further illustrate the possible mechanisms responsible for this increased antibacterial activity, Fig. 13 illustrates different possible interactions through which these nanomaterials interact and may disrupt pathogenic cells.

The antibacterial action of NPs involves several distinct mechanisms that may disrupt and halt cellular function in bacterial strains. Based on the literature review, we have proposed a possible mechanism to deactivate the bacterial cellular structure. Firstly, NPs may attach firmly to the surface of bacterial cells, compromising the integrity of the cell membrane; they may also penetrate the membrane and damage intra-

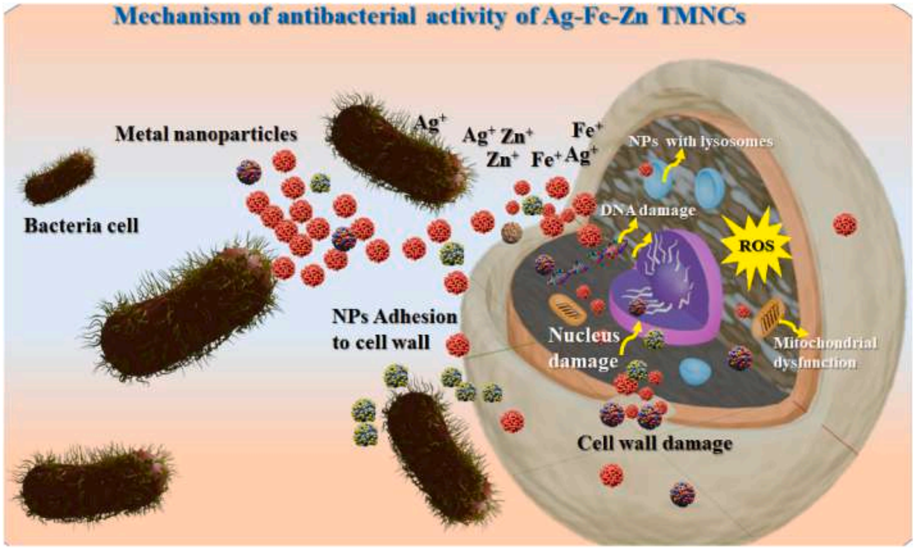

Fig. 13. The proposed possible mechanism model of antibacterial action of mono/BMNPs/TMNCs.

cellular structures. NPs may induce the production of reactive oxygen species (ROS) within the bacteria cell, which may cause cellular damage. Lastly, they may interfere with cellular signalling pathways, ultimately leading to cell inactivation and death. Advancing our comprehension of the molecular interactions and signalling pathways governing nanoparticle-cell membrane interfacial dynamics is critical for elucidating the underlying mechanisms of nanomaterial biocompatibility and cellular response [20,72,73]. The observed antibacterial activity of TMNCs highlights their promise, but further investigation using simulation and in vivo models is needed to assess their long-term efficacy and safety, as well as to explore how bacteria might adapt or develop resistance to these compounds.

The selective antibacterial activity of FeNPs and Zn-Fe BMNPs, which target EPEC (Gram-negative) but spare probiotic Lactobacillus (Gram-positive), likely stems from fundamental structural and physiological differences between these bacteria. The complex, lipopolysaccharide-rich outer membrane of Gram-negative pathogens may be more susceptible to disruption by metal ions and may facilitate nanoparticle penetration. In contrast, the dense, multi-layered peptidoglycan cell wall of Gram-positive bacteria like Lactobacillus could provide a robust protective barrier. Additional factors such as distinct membrane potentials, efflux pump efficiency, or differential oxidative stress response mechanisms may further contribute to this selectivity, highlighting the potential for targeted antimicrobial strategies that preserve beneficial microbiota.

In summary, this study highlights the unique advantages of Ag-Fe-Zn TMNCs, particularly their distinctive magnetic properties, which may open new avenues for targeted drug delivery in antibacterial applications. Notably, the Ag-Fe-Zn TMNCs demonstrated enhanced efficacy against *E. coli* pathogens while showing a favorable profile toward probiotic Lb species, suggesting their potential for selective antimicrobial therapy. These findings underscore the promise of Ag-Fe-Zn TMNCs as multifunctional agents, capable of both pathogen eradication and conservation of beneficial microbiota. While challenges remain in scaling up production, particularly in optimizing extract usage, metal salt concentrations, and synthesis control parameters, further research could focus on this aspects & facilitate broader clinical translation. Comparative studies with other MNP systems are warranted to fully establish the superior physicochemical stability and application-specific performance of Ag-Fe-Zn TMNCs. Overall, these insights pave the way for innovative, sustainable, and potentially useful targeted approaches to combat against resistant bacterial infections.

5. Conclusion

This study introduces a novel eco-friendly biosynthetic route for the fabrication of mono, bimetallic, and Ag-Fe-Zn trimetallic nanocomposites (TMNCs) utilizing TC leaf extract, with comprehensive characterization confirming their unique structural, magnetic, and optical properties. Among the synthesized nanoparticles, Ag-Fe BMNPs and Ag-Fe-Zn TMNCs stand out due to their distinctive magnetic properties, primarily attributed to the dominant $ZnFe_2O_4$ phase in the TMNCs and superior antibacterial efficacy, particularly against E. coli, while maintaining a selective profile that showed reduced impact to probiotic Lactobacillus (Lb) species. Comparative analysis revealed that & Ag-Fe-Zn TMNCs exhibited significantly greater antibacterial activity than their mono and bimetallic nanoparticles (BMNPs) counterparts, which is attributed to synergistic interactions among the constituent metal ions leading to effective membrane targeting, oxidative stress induction, and disruption of cellular signalling pathways. The combination of potent antibacterial action, magnetic behaviour, and selective targeting underscores the novelty and versatility of Ag-Fe-Zn TMNCs as a promising candidate for antimicrobial therapies with demonstrated selectivity towards beneficial microbiota. The magnetic behavior of these composites, combined with their antibacterial efficacy, positions them as promising candidates for future research into magnetically guided therapies. Further, this work encourages the exploration of their broader biomedical applications, including in vivo models, as well as anticancer and antitoxic effects, and supports their development as sustainable solutions in nanobiotechnology. Further exploration of the efficacy and safety profile of the TMNCs can be done using cytotoxicity tests and a better understanding of their anti-pathogenic activity and mechanistic pathways using vivo studies and models.

CRediT authorship contribution statement

Greeshma Sunkari: Data curation. **Saroj Vijaylakshmi:** Formal analysis, Data curation. **ML Sowjanya:** Data curation. **Vasamsetti Sai Madhuri:** Formal analysis, Data curation. **Naveen Kumar Madipoju:** Data curation, Conceptualization. **Naveen Kumar Dabbeta:** Data curation. **Prince Kumar:** Data curation. **Pranay Bhasker Kalakonda:** Methodology. **Likhith Chandan Kalakonda:** Visualization. **Vijay Morampudi:** Writing – review & editing, Supervision. **Suryanarayana Jammalamadaka:** Supervision, Methodology. **Parvathalu Kalakonda:** Writing – review & editing, Writing – original draft, Project administration, Investigation, Conceptualization.

Ethical approval

The internal review board committee of our lab stated that no ethical approval was required for this study as it did not involve human or animal subjects.

Funding

No funding was received for this project.

Declaration of interest statement

The authors declare that they have no known competing financial interests or personal relationships that could have appeared to influence the work reported in this paper- **Synergistic Antibacterial Activity of Green-Synthesized Ag-Fe-Zn Trimetallic Nanocomposites Using Tinospora Cordifolia Leaf Extract.**

Appendix A. Supplementary data

Supplementary data to this article can be found online at https://doi.org/10.1016/j.macse.2025.100048.

Data availability

The data supporting the findings of this study are available from the corresponding author upon reasonable request.

References

[1] N. Rarokar, S. Yadav, S. Saoji, P. Bramhe, R. Agade, S. Gurav, P. Khedekar, V. Subramaniyan, L.S. Wong, V. Kumarasamy, Magnetic nanosystem a tool for targeted delivery and diagnostic application: current challenges and recent advancement, Int. J. Pharm. X 7 (2024) 100231, https://doi.org/10.1016/j.ijpx.2024.100231.

[2] H. He, Q.-Q. Zhu, Y. Yan, H.-W. Zhang, Z.-Y. Han, H. Sun, J. Chen, C.-P. Li, Z. Zhang, M. Du, Metal–Organic Framework Supported Au Nanoparticles with Organosilicone Coating for High-Efficiency Electrocatalytic N2 Reduction to NH3, Appl. Catal. B Environ. 302 (2022) 120840, https://doi.org/10.1016/j.apcatb.2021.120840.

[3] H. Jiang, L. Li, Z. Li, X. Chu, Metal-based nanoparticles in antibacterial application in biomedical field: current development and potential mechanisms, Biomed. Microdevices 26 (1) (2024) 12, https://doi.org/10.1007/s10544-023-00686-8.

[4] S. Bhatia, Nanoparticles types, classification, characterization, fabrication methods and drug delivery applications, in: Natural Polymer Drug Delivery Systems, Springer International Publishing, Cham, 2016, pp. 33–93, https://doi.org/10.1007/978-3-319-41129-3_2.

[5] A.F. Burlec, A. Corciova, M. Boev, D. Batir-Marin, C. Mircea, O. Cioanca, G. Danila, M. Danila, A.F. Bucur, M. Hancianu, Current overview of metal nanoparticles' synthesis, characterization, and biomedical applications, with a focus on silver and gold nanoparticles, Pharmaceuticals 16 (10) (2023) 1410, https://doi.org/10.3390/ph16101410.

[6] S. Iravani, R.S. Varma, Green synthesis, biomedical and biotechnological applications of carbon and graphene quantum dots. A review, Environ. Chem. Lett. 18 (3) (2020) 703–727, https://doi.org/10.1007/s10311-020-00984-0.

[7] D. Sharma, S. Kanchi, K. Bisetty, Biogenic synthesis of nanoparticles: a review, Arab. J. Chem. 12 (8) (2019) 3576–3600, https://doi.org/10.1016/j.arabjc.2015.11.002.

[8] S. Ahmed, M. Ahmad, B.L. Swami, S. Ikram, A review on plants extract mediated synthesis of silver nanoparticles for antimicrobial applications: a green expertise, J. Adv. Res. 7 (1) (2016) 17–28, https://doi.org/10.1016/j.jare.2015.02.007.

[9] J. Singh, T. Dutta, K.-H. Kim, M. Rawat, P. Samddar, P. Kumar, 'Green' synthesis of metals and their oxide nanoparticles: applications for environmental remediation, J. Nanobiotechnol. 16 (1) (2018) 84, https://doi.org/10.1186/s12951-018-0408-4.

[10] C.L. Ventola, The antibiotic resistance crisis: part 1: causes and threats, P T 40 (4) (2015) 277–283.

[11] C. Sharma, S. Ansari, M.S. Ansari, S.P. Satsangee, M.M. Srivastava, Single-step green route synthesis of Au/Ag bimetallic nanoparticles using clove buds extract: enhancement in antioxidant bio-efficacy and catalytic activity, Mater. Sci. Eng. C 116 (2020) 111153, https://doi.org/10.1016/j.msec.2020.111153.

[12] C. Sharma, S. Ansari, M.S. Ansari, S.P. Satsangee, Phyto-mediated synthesis of Pt and Au/Pt bimetallic nanoparticles using Syzygium aromaticum bud-extract: study of their catalytic, antibacterial, and antioxidant activities, J. Ind. Eng. Chem. 111 (2022) 499–508, https://doi.org/10.1016/j.jiec.2022.04.031.

[13] P.M.Z. Hasan, C. Sharma, S. Ansari, M.S. Ansari, M.G. Alam, S.P. Satsangee, Eco-friendly fabrication of Ag/Pt bimetallic nanoparticles from clove extract: enhanced physicochemical properties and biomedical potential, Inorg. Chem. Commun. 174 (2025) 114086, https://doi.org/10.1016/j.inoche.2025.114086.

[14] T.M. Abdelghany, A.M.H. Al-Rajhi, M.A. Al Abboud, M.M. Alawlaqi, A. Ganash Magdah, E.A.M. Helmy, A.S. Mabrouk, Recent advances in green synthesis of silver nanoparticles and their applications: about future directions. A review, BioNanoScience 8 (1) (2018) 5–16, https://doi.org/10.1007/s12668-017-0413-3.

[15] K. Barman, P. Dutta, D. Chowdhury, P.K. Baruah, Green biosynthesis of copper oxide nanoparticles using waste Colocasia esculenta leaves extract and their application as recyclable catalyst towards the synthesis of 1,2,3-Triazoles, BioNanoScience 11 (1) (2021) 189–199, https://doi.org/10.1007/s12668-021-00826-5.

[16] P. Kalakonda, R. Kathi, M.G. Ligory, N. Dabbeta, N. Madipoju, S. Mynepally, V. Morampudi, S. Banne, P. Mandal, R.N. Savu, S.J. Khanam, M. Banavoth, N. V. Sudarsanam Eve, B.B. Podila, Argyreia nervosa-driven biosynthesis of Cu–Ag bimetallic nanoparticles from plant leaves extract unveils enhanced antibacterial properties, Bioproc. Biosyst. Eng. 47 (8) (2024) 1307–1319, https://doi.org/10.1007/s00449-024-03020-5.

[17] P. Kalakonda, P. Mandal, S. Laxmi Mynepally, A. Bashipangu, A. Kethavath, S. J. Khanam, M. Batchu, P.B. Kalakonda, S. Banne, D. Aitipamula, M. Banavoth, M. Kigoji, V.D. Shukla, Y. Eluri, B.B. Podila, Comparison of multi-metallic nanoparticles-alternative antibacterial agent: understanding the role of their antibacterial properties, J. Inorg. Organomet. Polym. 34 (5) (2024) 2203–2218, https://doi.org/10.1007/s10904-023-02960-x.

[18] P. Singh, Y.-J. Kim, D. Zhang, D.-C. Yang, Biological synthesis of nanoparticles from plants and microorganisms, Trends Biotechnol. 34 (7) (2016) 588–599, https://doi.org/10.1016/j.tibtech.2016.02.006.

[19] K. Jyoti, M. Baunthiyal, A. Singh, Characterization of silver nanoparticles synthesized using Urtica Dioica Linn. Leaves and their synergistic effects with antibiotics, Journal of Radiation Research and Applied Sciences 9 (3) (2016) 217–227.

[20] M. Arakha, S. Pal, D. Samantarrai, T.K. Panigrahi, B.C. Mallick, K. Pramanik, B. Mallick, S. Jha, Antimicrobial activity of iron oxide nanoparticle upon modulation of nanoparticle-bacteria interface, Sci. Rep. 5 (1) (2015) 14813, https://doi.org/10.1038/srep14813.

[21] C. Verma, D.K. Verma, E. Berdimurodov, I. Barsoum, A. Alfantazi, C.M. Hussain, Green magnetic nanoparticles: a comprehensive review of recent progress in biomedical and environmental applications, J. Mater. Sci. 59 (2) (2024) 325–358.

[22] M. Chandra Sekhar, B. Purusottam Reddy, C. Kuchi, C. Kamal Basha, F.A.M. Al-Zahrani, R. Mangiri, Enhanced solar-driven photocatalytic hydrogen production, dye degradation, and supercapacitor functionality using MoS2–TiO2 nanocomposite, Ceram. Int. 50 (20) (2024) 38679–38687, https://doi.org/10.1016/j.ceramint.2024.07.239.

[23] R. Mangiri, T. Ramachandran, Y.A. Kumar, A. Ghosh, A.G. Al-Sehemi, A.K. Yadav, D. Mani, Surface engineering of M5X4 MXenes for next-gen energy solutions, Mater. Today Chem. 48 (2025) 102864, https://doi.org/10.1016/j.mtchem.2025.102864.

[24] Akl M. Awwad, M.W. Amer, Nidà M. Salem, Amany O. Abdeen, Green synthesis of zinc oxide nanoparticles (ZnO-NPs) using Ailanthus Altissima fruit extracts and antibacterial activity. https://doi.org/10.5281/ZENODO.3559520, 2020.

[25] A. Ed-Dra, E.M. Abdallah, A.M.E. Sulieman, H. Anarghou, Harnessing medicinal plant compounds for the control of campylobacter in foods: a comprehensive review, Vet. Res. Commun. 48 (5) (2024) 2877–2900, https://doi.org/10.1007/s11259-024-10455-4.

[26] I.M. Idowu, T.-X. Li, E.A. Orgah, J.O. Thomas, K.O. Olaniyan, Y.-Z. Chen, A. Oguntoyinbo, S.G. Rudrapatna, Harnessing medicinal plants: new hope for typhoid fever antibacterial agents - mini review, Nat Ther Adv 8 (1) (2025) 3, https://doi.org/10.53388/NTA2025003.

[27] L.M. Dwivedi, N. Shukla, K. Baranwal, S. Gupta, S. Siddique, V. Singh, Gum Acacia modified Ni doped CuO nanoparticles: an excellent antibacterial material, J. Cluster Sci. 32 (1) (2021) 209–219, https://doi.org/10.1007/s10876-020-01779-7.

[28] K. Nagaraja, M. Arunpandian, O. Tae Hwan, A facile green synthesis of manganese oxide nanoparticles using gum karaya polymer as a bioreductant for efficient photocatalytic degradation of organic dyes and antibacterial activity, Int. J. Biol. Macromol. 273 (2024) 133123, https://doi.org/10.1016/j.ijbiomac.2024.133123.

[29] S. Iravani, Green synthesis of metal nanoparticles using plants, Green Chem. 13 (10) (2011) 2638–2650.

[30] A. Vinukonda, N. Bolledla, R.K. Jadi, R. Chinthala, V.R. Devadasu, Synthesis of nanoparticles using advanced techniques, Nanotechnology 8 (2025) 100169.

[31] S. Das, B. Sen, N. Debnath, Recent trends in nanomaterials applications in environmental monitoring and remediation, Environ. Sci. Pollut. Control Ser. 22 (23) (2015) 18333–18344.

[32] A.S. Adeleye, J.R. Conway, K. Garner, Y. Huang, Y. Su, A.A. Keller, Engineered nanomaterials for water treatment and remediation: costs, benefits, and applicability, Chem. Eng. J. 286 (2016) 640–662, https://doi.org/10.1016/j.cej.2015.10.105.

[33] A. Baranwal, A. Srivastava, P. Kumar, V.K. Bajpai, P.K. Maurya, P. Chandra, Prospects of nanostructure materials and their composites as antimicrobial agents, Front. Microbiol. 9 (2018) 422, https://doi.org/10.3389/fmicb.2018.00422.

[34] P. Kalakonda, Synthesis of silver nanowires for highly conductive and transparent films, Nanomater. Nanotechnol. 6 (2016) 1847980416663672.

[35] P. Kalakonda, B. Sreenivas, Synthesis and optical properties of highly stabilized peptide-coated gold nanoparticles, Plasmonics 12 (4) (2017) 1221–1225.

[36] P. Kalakonda, S. Banne, Synthesis and optical properties of highly stabilized peptide-coated silver nanoparticles, Plasmonics 13 (4) (2018) 1265–1269.

[37] E.M. Abdallah, B.Y. Alhatlani, R. De Paula Menezes, C.H.G. Martins, Back to nature: medicinal plants as promising sources for antibacterial drugs in the post-antibiotic era, Plants 12 (17) (2023) 3077, https://doi.org/10.3390/plants12173077.
[38] K. Parvathalu, K. Rajitha, B. Chandrashekar, K. Sathvik, K. Pranay Bhasker, B. Sreenivas, M. Pritam, P. Pushpalatha, K. Moses, P. Bala Bhaskar, Biomimetic synthesis of copper nanoparticles using Tinospora Cordifolia plant leaf extract for photocatalytic activity applications, Plasmonics 19 (2) (2024) 825–834.
[39] A. Bassi, P. Kalakonda, I. Hasan, Synthesis of Chitosan-Agar immobilized NiO-MgO bionanocomposites and their photocatalytic application towards toxic Azo dye, Inorg. Chem. Commun. 170 (2024) 113499.
[40] E.V. Araújo, S.V. Carneiro, D.M.A. Neto, T.M. Freire, V.M. Costa, R.M. Freire, L. Fechine, C.S. Clemente, J.C. Denardin, J.C.S. Dos Santos, Advances in surface design and biomedical applications of magnetic nanoparticles, Adv. Colloid Interface Sci. 328 (2024) 103166.
[41] R.N. Morgan, K.M. Aboshanab, Green biologically synthesized metal nanoparticles: biological applications, optimizations and future prospects, Future Science OA 10 (1) (2024) FSO935.
[42] D.-M. Radulescu, V.-A. Surdu, A. Ficai, D. Ficai, A.-M. Grumezescu, E. Andronescu, Green synthesis of metal and metal oxide nanoparticles: a review of the principles and biomedical applications, Int. J. Mol. Sci. 24 (20) (2023) 15397.
[43] J. Rani, T. Goyal, A. Kaur, S. Ganesan, A.K. Sharma, A.S. Chauhan, S. Kumar, S. Kaushal, Bimetallic nanoparticles as pioneering eco-friendly catalysts for remediation of pharmaceuticals and personal care products (PPCPs), Nanoscale Adv. (2025).
[44] C.P. Devatha, A.K. Thalla, S.Y. Katte, Green synthesis of iron nanoparticles using different leaf extracts for treatment of domestic waste water, J. Clean. Prod. 139 (2016) 1425–1435.
[45] N.K. Madipoju, S.J. Khanam, G. Sunkari, S.M. Vasamsetti, V. Divyasri, V. Morampudi, R.N. Savu, M. Banavoth, S. Banne, I. Hasan, Bimetallic zinc-silver nanocomposites for superior antimicrobial efficacy, Appl. Phys. A 131 (2) (2025) 153.
[46] I. Hasan, A. Bassi, P. Kalakonda, CuO surface functionalized β-Cyclodextrin grafted PMMA hybrid nanocomposite for advance oxidative mineralization of Methyl Orange, Surf. Interfaces 56 (2025) 105456.
[47] P. Kalakonda, R. Kathi, M.G. Ligory, N. Dabbeta, N. Madipoju, S. Mynepally, V. Morampudi, S. Banne, P. Mandal, R.N. Savu, Argyreia nervosa-driven biosynthesis of Cu–Ag bimetallic nanoparticles from plant leaves extract unveils enhanced antibacterial properties, Bioproc. Biosyst. Eng. 47 (8) (2024) 1307–1319.
[48] P. Kalakonda, A. Bashitangu, P. Mandal, S. Jowhar Khanam, M. Banovath, I. Hasan, B. Bhaskar Podila, Sustainable solutions for clean water: green synthesized cu-ag-bimetallic nanoparticles based Nano catalyst, Mater. Sci. Eng., B 301 (2024) 117147, https://doi.org/10.1016/j.mseb.2023.117147.
[49] K. Parvathalu, D.N. Kumar, K. Rajitha, M.G. Kishan, B.N. Kumar, J. Bhemarajam, S. R. Naidu, G.L. Merlinsheeba, P. Mandal, S. Banne, Facile synthesis of silver nanoparticles using green tea leaf extract and evolution of antibacterial activity, Plasmonics 18 (5) (2023) 1837–1845.
[50] P. Kalakonda, M.A. Aldhahri, M.S. Abdel-Wahab, A. Tamayol, K.M. Moghaddam, F. B. Rached, A. Pain, A. Khademhosseini, A. Memic, S. Chaieb, Microfibrous silver-coated polymeric scaffolds with tunable mechanical properties, RSC Adv. 7 (55) (2017) 34331–34338.
[51] R.B. Asamoah, A. Yaya, B. Mensah, P. Nbalayim, V. Apalangya, Y.D. Bensah, L.N. W. Damoah, B. Agyei-Tuffour, D. Dodoo-Arhin, E. Annan, Synthesis and characterization of zinc and copper oxide nanoparticles and their antibacteria activity, Results Mater. 7 (2020) 100099.
[52] Y. Cao, H.A. Dhahad, M.A. El-Shorbagy, H.Q. Alijani, M. Zakeri, A. Heydari, E. Bahonar, M. Slouf, M. Khatami, M. Naderifar, Green synthesis of bimetallic ZnO–CuO nanoparticles and their cytotoxicity properties, Sci. Rep. 11 (1) (2021) 23479.
[53] M. Darvish, N. Nasrabadi, F. Fotovat, S. Khosravi, M. Khatami, S. Jamali, E. Mousavi, S. Iravani, A. Rahdar, Retracted article: biosynthesis of Zn-Doped CuFe2O4 nanoparticles and their cytotoxic activity, Sci. Rep. 12 (1) (2022) 9442.
[54] E.A. Mohamed, Green synthesis of copper & copper oxide nanoparticles using the extract of seedless dates, Heliyon 6 (1) (2020) e03123.
[55] S.P. Dubey, M. Lahtinen, M. Sillanpää, Tansy fruit mediated greener synthesis of silver and gold nanoparticles, Process Biochem. 45 (7) (2010) 1065–1071.
[56] X. Jiang, S. Li, G. Xiang, Q. Li, L. Fan, L. He, K. Gu, Determination of the acid values of edible oils via FTIR spectroscopy based on the OH stretching band, Food Chem. 212 (2016) 585–589.
[57] S.A. Khan, S.B. Khan, L.U. Khan, A. Farooq, K. Akhtar, A.M. Asiri, Fourier transform infrared spectroscopy: fundamentals and application in functional groups and nanomaterials characterization, in: Handbook of Materials Characterization, Springer, 2018, pp. 317–344.
[58] P. Tyagi, A.K. Chauhan, Optimization and characterization of functional cookies with addition of Tinospora cordifolia as a source of bioactive phenolic antioxidants, Lebensm. Wiss. Technol. 130 (2020) 109639.
[59] I.A.M. Ali, A.B. Ahmed, H.I. Al-Ahmed, Green synthesis and characterization of silver nanoparticles for reducing the damage to sperm parameters in diabetic compared to metformin, Sci. Rep. 13 (1) (2023) 2256.
[60] S. Shahzadi, S. Fatima, Z. Shafiq, M.R.S.A. Janjua, A review on green synthesis of silver nanoparticles (SNPs) using plant extracts: a multifaceted approach in photocatalysis, environmental remediation, and biomedicine, RSC Adv. 15 (5) (2025) 3858–3903.
[61] S.I. Manzoor, F. Jabeen, R. Patel, M.M. Alam Rizvi, K. Imtiyaz, M.A. Malik, T. A. Dar, Green synthesis of biocompatible silver nanoparticles using *Trillium Govanianum* rhizome extract: comprehensive biological evaluation and *in Silico* analysis, Mater. Adv. 6 (2) (2025) 682–702, https://doi.org/10.1039/D4MA00959B.
[62] P. Kumar, J. Asokan, S. Sriram, M.C. Ramkumar, P.S. Kumar, M.G. Shalini, Impact of annealing on $ZnFe_2O_4$: structural, optical, magnetic, photocatalytic, and antibacterial properties with DFT insights into optical parameters, J. Hazardous Mater. Adv. 17 (2025) 100594, https://doi.org/10.1016/j.hazadv.2025.100594.
[63] D. Cao, H. Li, L. Pan, J. Li, X. Wang, P. Jing, X. Cheng, W. Wang, J. Wang, Q. Liu, High saturation magnetization of γ-Fe2O3 nano-particles by a facile one-step synthesis approach, Sci. Rep. 6 (1) (2016) 32360, https://doi.org/10.1038/srep32360.
[64] Dhaka S. Garima, M. Panda, V. Singh, P. Prajapat, B.L. Choudhary, S. Kumar, Tailoring the structural and dielectric properties of ZnFe2O4 through annealing temperature, Phys. B Condens. Matter 674 (2024) 415574, https://doi.org/10.1016/j.physb.2023.415574.
[65] N.T.T. Tu, T.L.-A. Vo, T.T.-T. Ho, K.-P.T. Dang, V.-D. Le, P.N. Minh, C.-H. Dang, V.-T. Tran, V.-S. Dang, T.T.K. Chi, H. Vu-Quang, R. Fajgar, T.-L.-H. Nguyen, V.-D. Doan, T.-D. Nguyen, Silver nanoparticles loaded on Lactose/Alginate: in situ synthesis, catalytic degradation, and pH-Dependent antibacterial activity, Beilstein J. Nanotechnol. 14 (2023) 781–792, https://doi.org/10.3762/bjnano.14.64.
[66] D.J. Pochapski, C. Carvalho Dos Santos, G.W. Leite, S.H. Pulcinelli, C.V. Santilli, Zeta potential and colloidal stability predictions for inorganic nanoparticle dispersions: effects of experimental conditions and electrokinetic models on the interpretation of results, Langmuir 37 (45) (2021) 13379–13389, https://doi.org/10.1021/acs.langmuir.1c02056.
[67] A. Bhardwaj, A.K. Singh, Green synthesis of magnetic Fe–Co bimetallic nanoparticles and their photocatalytic activity, Appl. Nanosci. 5 (3) (2024) 108–115, https://doi.org/10.3390/applnano5030009.
[68] Y. Yan, G. Li, M. Su, H. Liang, *Scutellaria Baicalensis* polysaccharide-mediated green synthesis of smaller silver nanoparticles with enhanced antimicrobial and antibiofilm activity, ACS Appl. Mater. Interfaces 16 (34) (2024) 45289–45306, https://doi.org/10.1021/acsami.4c07770.
[69] N.T. Tasnim, N. Ferdous, Md M.H. Rumon, M.S. Shakil, The promise of metal-doped iron oxide nanoparticles as antimicrobial agent, ACS Omega 9 (1) (2024) 16–32, https://doi.org/10.1021/acsomega.3c06323.
[70] M.U. Rashid, S.J. Shah, S. Attacha, L. Khan, J. Saeed, S.T. Shah, H.I. Mohamed, Green synthesis and characterization of zinc oxide nanoparticles using citrus Limetta peels extract and their antibacterial activity against brown and soft rot pathogens and antioxidant potential, Waste Biomass Valor 15 (6) (2024) 3351–3366, https://doi.org/10.1007/s12649-023-02389-w.
[71] J. Ji, Q. Zhang, H. Mo, Z. Ren, Y. Lin, Z. Chen, T. Leiviskä, Z. Wu, Plant-cell mediated synthesis of MnCo2O4 nanoparticles and their activation of peroxymonosulfate to remove tetracycline, Chem. Eng. J. 492 (2024) 152212, https://doi.org/10.1016/j.cej.2024.152212.
[72] Y.N. Slavin, J. Asnis, U.O. Häfeli, H. Bach, Metal nanoparticles: understanding the mechanisms behind antibacterial activity, J. Nanobiotechnol. 15 (1) (2017) 65, https://doi.org/10.1186/s12951-017-0308-z.
[73] A.A. Akinsiku, R.O. Odaudu, O.C. De Campos, A.O. Adeyemi, O. Ejilude, Synthesis of low toxic silver-cobalt nanoparticles using Annona Muricata leaf extract: antimicrobial evaluation, Inorg. Chem. Commun. 153 (2023) 110837, https://doi.org/10.1016/j.inoche.2023.110837.